# Multi-wavelength Čerenkov radiations in a microring resonator in combination with two gratings*

**Rangsan Jomtarak[1,2] and Preecha P. Yupapin[2,3,4]**

1. *Faculty of Science and Technology, Suan Dusit Rajabhat University, Bangkok 10700, Thailand*
2. *Advanced Studies Center, Department of Physics, Faculty of Science, King Mongkut's Institute of Technology Ladkrabang (KMITL), Bangkok 10520, Thailand*
3. *Interdisciplinary Research Center, Faculty of Science and Technology, Kasem Bundit University, Bangkok 10250, Thailand*
4. *Spintronics Research Center, Department of Physics, Faculty of Science, Kasetsart University, Bangkok 10900, Thailand*

(Received 24 April 2015)


In this paper, the Čerenkov radiation of light pulse in a microring and gratings is simulated and investigated. The system design consists of a two-defect grating incorporating a microring, connected with a uniform grating. In simulation, the continuous wave (CW) light pulse with wavelength centered at 1.55 μm is input into the microring device via the two-defect grating. The resonant outputs from the two-defect grating propagate through the microring and uniform grating, where the time delays of those two input pulses with different wavelengths through the system are distinguished by the output uniform grating. From the obtained resonant output pulses, we find that the red-shifted and blue-shifted Čerenkov pulses are observed. In applications, such a proposed system can be used to form two different optical delay pulses, in which the change in Čerenkov radiation of them, i.e., time delay within a microring device system, can be useful for Čerenkov radiation imaging and sensing applications.

**Document code:** A **Article ID:** 1673-1905(2015)04-0252-4
**DOI** 10.1007/s11801-015-5069-z

Čerenkov radiation is one of the signals produced by interactions between charged particles and medium[1,2]. Čerenkov radiation has been studied theoretically and experimentally in one-dimensional periodic multilayer stacks[3], photonic crystals[1,4], fiber optics[2,5,6], channel waveguide[7,8], coaxial slow-wave structure[9], photonic crystal fiber[10], bulk birefringent quadratic medium[11] and metamaterials[12].

In applications, many forms of Čerenkov radiation were used in various works. A fiber-optic Čerenkov radiation sensor without an organic scintillator was employed to measure the Čerenkov radiation induced by therapy as a function of the dose rate of the proton beams[13,14]. The Čerenkov detector for half-value layer (HVL) measurement with detection threshold in the low energy range was formed by the industrial electron linear accelerators (LINACs)[15]. Čerenkov luminescence light signal from radionuclides was applied for nuclear imaging[16]. The optical fibers were designed to be the Čerenkov detector for imaging in radiation therapy[17]. The Čerenkov radiation generated in the fiber-optic radiation sensor by irradiation of pure thermal neutron beams was measured in different depths of polyethylene for detecting thermal neutrons in high-temperature conditions[18]. Recently, we have shown that the red-shifted and blue-shifted Čerenkov radiation could be generated by using the optical light pulse traveling through the nested nonlinear microring resonators and gratings system[19]. In this paper, a simple scheme of Čerenkov radiation is proposed. It can be found that the red-shifted and blue-shifted Čerenkov radiation can be generated and distinguished within the small scale optical device, which is useful for various applications, such as Čerenkov sensing and imaging and fast and slow light, in which the small scale sensing device can be fabricated and employed.

The proposed Čerenkov radiation system is shown in Fig.1, which consists of a two-defect grating incorporating a microring and a uniform grating at the output port. The amplitude of electric field $E_j$ inside the $j$th layer can be written as[20]

$$E_j = E_{\mathrm{F}j} \exp[-\mathrm{i}k_j z + \mathrm{i}\varphi_{\mathrm{F}j}(z)] + E_{\mathrm{B}j} \exp[\mathrm{i}k_j z + \mathrm{i}\varphi_{\mathrm{B}j}(z)], \quad (1)$$

* E-mail: panda.yupapin@gmail.com

where $E_{Fj}$ and $E_{Bj}$ are the amplitudes of the forward and backward propagating waves in the $j$th layer, respectively. $\varphi_{Fj}$ and $\varphi_{Bj}$ are the nonlinear induced phase changes of the forward and backward propagating waves in the $j$th layer, respectively. The amplitudes of the forward and backward propagating waves in the $j$th layer are related to those in the layer $j$+1 by a matrix, which is given by[20]

$$\begin{pmatrix} E_{Fj} \\ E_{Bj} \end{pmatrix} = \begin{pmatrix} \frac{k_j + k_{j+1}}{2k_j} e^{2ik_j L_j} & \frac{k_j + k_{j+1}}{2k_j} e^{2i(k_j + k_{j+1})L_j} \\ \frac{k_j + k_{j+1}}{2k_j} e^{-[\varphi_{Bj}(L_j) - \varphi_{Fj}(L_j)]} & \frac{k_j + k_{j+1}}{2k_j} e^{2ik_{j+1}L_j - i[\varphi_{Bj}(L_j) - \varphi_{Fj}(L_j)]} \end{pmatrix} \begin{pmatrix} E_{Fj+1} \\ E_{Bj+1} \end{pmatrix} \quad (2)$$

where $L_j$ is the ending $z$-coordinate of the $j$th layer, and $k_j$ is the wave number in the $j$th layer. Since the $n$+1 layer extends to infinity, there is no backward propagating wave in this layer. By working backward, we can calculate the amplitude in the $n$th layer and other preceding layers from the outgoing wave $E_T$, so the incident wave is related to the transmitted wave[20].

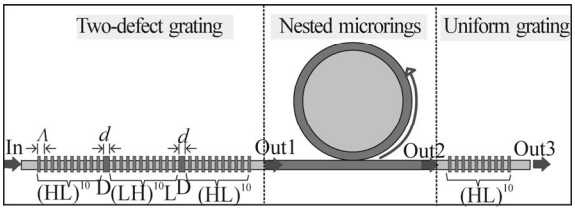


**Fig.1 Schematic diagram of the Čerenkov radiation system consisting of microring and gratings, where $\Lambda$=0.2 μm, $d_H$=0.1 μm for InP material, $d_L$=0.08 μm for InGaAsP material, and $d_D$=0.2 μm for GaAs material**

The simulation parameters are fixed by the refractive index of waveguide $n_H$=3.51 for InGaAsP material. The radius of microring is 3.1 μm. The lower layer uses the InP material with the refractive index $n_L$=3.22, where the nonlinear refractive index coefficient is $2.2\times10^{-13}$ m$^2$/W (InGaAsP/InP). Simulation results are obtained by using the finite difference time domain (FDTD) method (Optiwave@OptiFDTD), which is a commercial software program, and the used device parameters are chosen close to the practical fabrication parameters. Results of output intensity are shown in Fig.2(a), and we find that the output intensity at out1 is higher than those at out2 and out3. The output intensity at the wavelength of 1.65 μm is red-shifted, which is caused by the forward emissions of optical waveguide layers[21], for instance, the two-defect modes. This shifted result in Fig.2(a) is confirmed by the conversion of output power as shown in Fig.2(b).

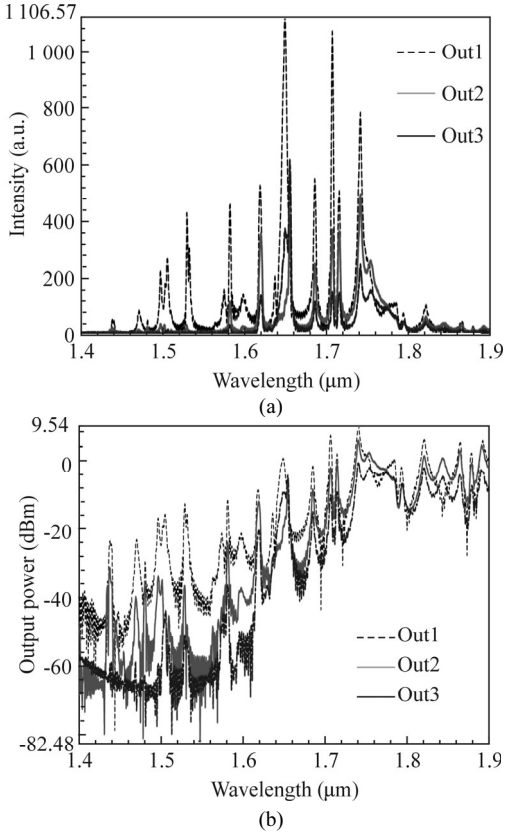


**Fig.2 Simulation results of (a) output intensity and (b) output power of the light pulse propagation through the designed model, where the center wavelength of input light pulse is 1.55 μm**

Additionally, the shifted output intensity depends on the incident light pulse at the input waveguide, which is shown in Fig.3. We find that when the incident light pulse is changed from 0° to 10°, $\Delta\lambda$=10 nm. The reflection (blue-shifted) of the produced radiation from the interfacing layers is now properly taken into account, and Fig.4 shows the absorption of Čerenkov radiation due to the passage of fast photons (or trapped particles, i.e., electrons) through the device layer. It can be seen from Fig.4 that the blue-shifted radiation and red-shifted radiation occur at the center wavelengths of 1.395 μm (215 THz) and 1.714 μm (175 THz) for the input wavelength centered at 1.55 μm, respectively.

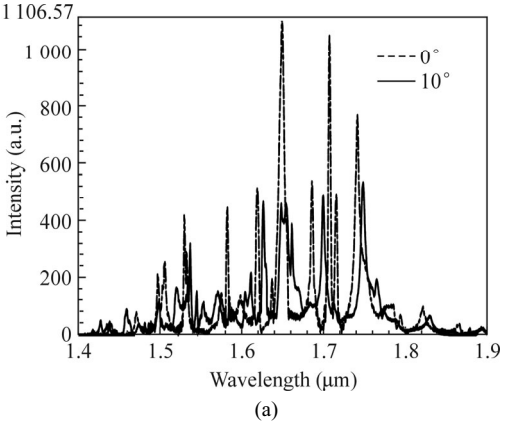

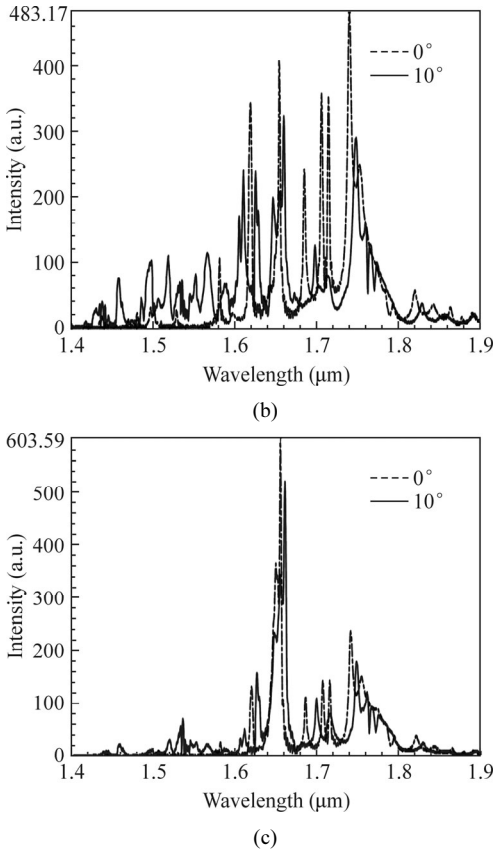


**Fig.3 Simulation results of output intensity at (a) out1, (b) out2 and (c) out3 with the incident angles of light pulse of 0° and 10°, where the center wavelength of input light pulse is 1.55 μm**

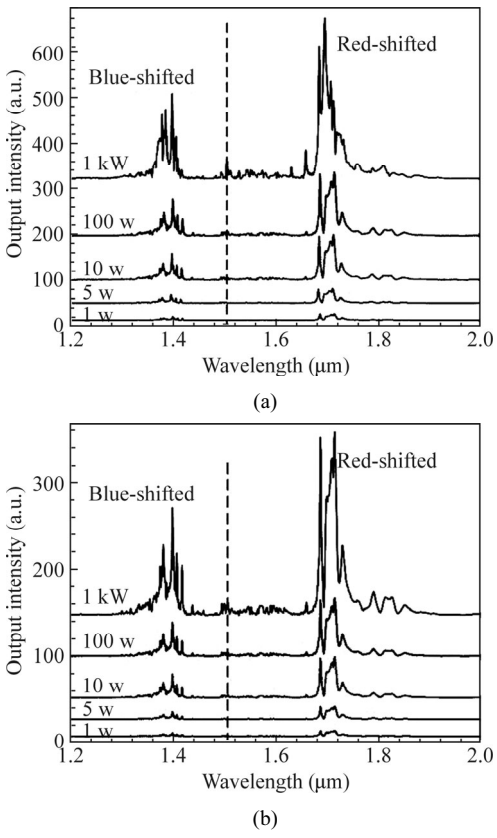


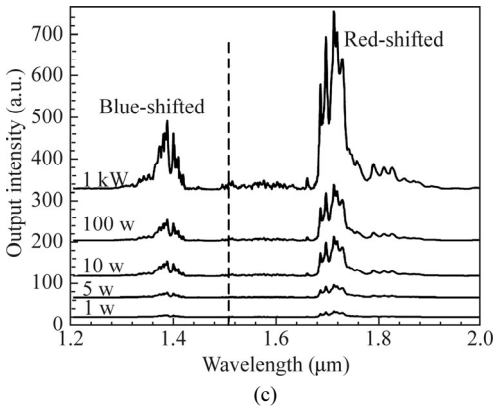


**Fig.4 Results of Čerenkov effects at (a) out1, (b) out2 and (c) out3 with input pump pulse at center wavelength of 1.55 μm for red-shifted and blue-shifted radiation**

In Fig.5, the electrical field intensity propagating in $y$ direction with full width at half maximum (FWHM) of 0.375 μm through the optical waveguide system is demonstrated, and the center wavelength of the input CW optical light pulse is 0.785 5 μm. In Fig.6, the simulation result of the input light pulse with center wavelength of 785.5 nm and FWHM of $1.05\times10^{-13}$ s is obtained. In Fig.6(b), the normalized output at the out1 is plotted for blue-shifted Čerenkov radiation, in which the blue-shifted Čerenkov results have 6 output wavelengths of 766.72 nm, 771.09 nm, 787.33 nm, 793.01 nm, 798.40 nm and 814.21 nm, respectively, as shown in the inset of Fig.6(b).

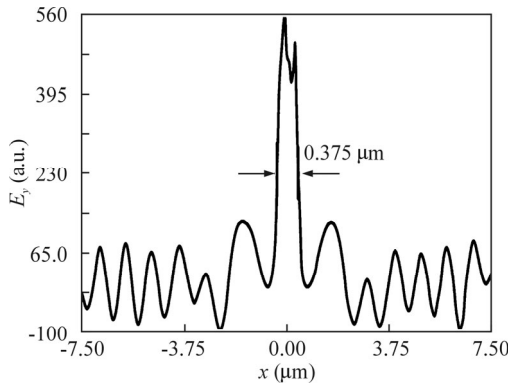


**Fig.5 Output $E_y$ versus position within the system, where the center wavelength of input light pulse is 1.55 μm**

The forward and backward light pulses with two-defect modes in two-defect grating are absorbed and emitted by this center wavelength. In Fig.6(c), the normalized output of red-shifted Čerenkov radiation after light passing through the microring at the out2 is plotted. There are 12 blue-shifted Čerenkov radiation wavelengths as shown in inset of Fig.6(c), which are 752.08 nm, 757.03 nm, 761.98 nm, 766.57 nm, 771.23 nm, 776.19 nm, 781.72 nm, 787.48 nm, 793.01 nm, 803.06 nm, 808.75 nm and 814.14 nm, respec-

tively. In Fig.6(d), the combination (interference filter) between red-shifted and blue-shifted Čerenkov radiations is filtered by the uniform grating at the out3, where the normalized outputs are at 752.15 nm, 757.10 nm, 761.91 nm, 766.57 nm, 771.16 nm, 776.19 nm, 781.80 nm, 787.48 nm, 793.01 nm, 797.89 nm, 803.29 nm, 808.67 nm and 813.92 nm, respectively, as shown in the inset of Fig.6(d).

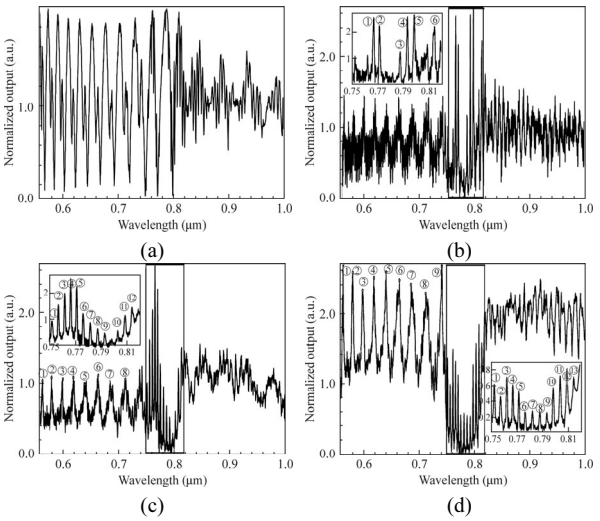


**Fig.6 (a) Input light pulse with center wavelength at 0.785 5 μm; Results of the normalized outputs at (b) out1 (inset: blue-shifted Cerenkov radiation), (c) out2 (inset: red-shifted Čerenkov radiation), and (d) out3**

The Čerenkov radiation of optical pulse in a microring system is simulated and presented. The output signals confirm that the shifted particle (photon) speed can be obtained, the shock optical wave behavior is observed, and the two different optical pulse time delays can be arranged. In this paper, the blue-shifted radiation and red-shifted radiation occur at the center wavelengths of 1.395 μm (215 THz) and 1.714 μm (175 THz) for the input wavelength centered at 1.55 μm, respectively. Regarding the present fabrication and the signal detection technologies, using luminescence light signal and device (microring) for Čerenkov radiation sensing and imaging applications is reasonable.

**Acknowledgments**

R. Jomtarak acknowledges Suan Dusit Rajabhat University, Bangkok, Thailand for granting the Thailand Ph.D. Program at Department of Physics, Faculty of Science, King Mongkut's Institute of Technology Ladkrabang (KMITL), Bangkok 10520, Thailand.

## References

[1] C. Luo, M. Ibanescu, S. G. Johnson and J. D. Joannopoulos, Science **299**, 368 (2003).

[2] J. H. Lee, J. van Howe, C. Xu and X. Liu, IEEE Journal of Selected Topics in Quantum Electronics **14**, 713 (2008).

[3] B. Lastdrager, A. Tip and J. Verhoeven, Physical Review E **61**, 5767 (2000).

[4] K. Kalinowski, V. Roppo, T. Łukasiewicz, M. Świrkowicz, Y. Sheng and W. Krolikoaski, Applied Physics B **109**, 557 (2012).

[5] J. Cheng, J. H. Lee, K. Wang, C. Xu, K. G. Jespersen, M. Garmund, L. Grüner-Nielsen and D. Jakobsen, Optics Express **19**, 8774 (2011).

[6] B. Lee, K. W. Jang, W. J. Yoo, S. H. Shin, J. Moon, K.-T. Han and D. Jeon, IEEE Transactions on Nuclear Science **60**, 932 (2013).

[7] G. L. Du, G. Q. Li, S. Z. Zhao, T. Li and X. Li, Optik-International Journal for Light and Electron Optics **123**, 896 (2012).

[8] G. Du, G. Li, S. Zhao, X. Li and Z. Yu, Optics & Laser Technology **44**, 830 (2012).

[9] X. Renzhen, L. Yuzheng, S. Zhimin, C. Changhua and L. Guozhi, IEEE Transactions on Plasma Science **35**, 145 (2007).

[10] S. A. Dekker, A. C. Judge, R. Pant, I. Gris-Sánchez, J. C. Knight, C. M. de Sterke and B. J. Eggleton, Optics Express **19**, 17766 (2011).

[11] W. Wang, Y. Sheng, X. Niu, M. Huang, S. Zheng and Y. Kong, Optics & Laser Technology **58**, 16 (2014).

[12] H. Chen and M. Chen, Materials Today **14**, 34 (2011).

[13] W. J. Yoo, S. H. Shin, D. Jeon, S. Hong, S. G. Kim, H. I. Sim, K. W. Jang, S. Cho and B. Lee, Optics Express **21**, 27770 (2013).

[14] K. W. Jang, W. J. Yoo, S. H. Shin, D. Shin and B. Lee, Optics Express **20**, 13907 (2012).

[15] S. Li, K. Kang, Y. Wang, J. Li, J.-J. Song and Y. Li, Radiation Measurements **46**, 726 (2011).

[16] C. Qin, J. Zhong, Z. Hu, X. Yang and J. Tian, IEEE Journal of Selected Topics Quantum Electronics **18**, 1084 (2012).

[17] I. Silva and G. Pang, Radiation Physics Chemistry **81**, 599 (2012).

[18] K. W. Jang, T. Yagi, C. H. Pyeon, W. J. Yoo, S. H. Shin, T. Misawa and B. Lee, Optics Express **21**, 14573 (2013).

[19] R. Jomtarak and P. P. Yupapin, Journal of the Optical Society America B **31**, 474 (2014).

[20] X. Li, K. Xie and H.-M. Jiang, Optics Communications **282**, 4292 (2009).

[21] M. Cheng, Optics Express **15**, 9793 (2007).